Available online at www.sciencedirect.com

ScienceDirect

Procedia CIRP 00 (2018) 000–000

www.elsevier.com/locate/procedia

12th CIRP Conference on Intelligent Computation in Manufacturing Engineering, 18-20 July 2018, Gulf of Naples, Italy

A Vibration Control for Disassembly of Turbine Blades

Santiago D. Mullo[a], Edwin Pruna[a], Julius Wolff[b]*, Annika Raatz[b]

[a]*Universidad de las Fuerzas Armadas ESPE, Sangolqui, Ecuador*

[b]*Institute of Assembly Technology, An der Universität 2, Leibniz Universität Hannover, 30823 Garbsen, Germany*

* Corresponding author. Tel.: +49-(0)511-762-18248; fax: +49-(0)511-762-18251. *E-mail address:* wolff@match.uni-hannover.de

Abstract

Typically disassembly forces are unknown due to high forces or high temperatures during product operation, so that assembly connections solidify. For controlling the disassembly forces a control is developed. The controller is formed for two steps: The first step is a control by a PID controller that produces a force, which overcomes a solidifying force slightly. The second step is a vibration control with a FM modulation for controlling the duration of impacts. Vibrations are useful for decreasing the force amplitude for caring the joined components. Finally, the control is validated with disturbances in a simulation.

Peer-review under responsibility of the scientific committee of the 12th CIRP Conference on Intelligent Computation in Manufacturing Engineering.

Keywords: Disassembly; Force Control; Friction Model; Vibration Control

1. Introduction

Many industries such as aircraft consume scare resources generating pollution that impacts across entire product life cycle from raw material to its final disposal producing high environmental loads. The life cycle of a product begins with the extraction of the raw material, after which it enters the preparation or assembly phase, then follows the use phase follows, some products go through a maintenance or repair phase, when a product has reached the end of its life cycle is discarded or recycled [1].

Some of the materials in aircraft are costly to produce, mainly in engines, since they are made of materials such as composites and alloys with very high mechanical strength and resistance to high temperatures and corrosion [2]. These parts, like the turbine blades are subjected to rapid heating and cooling during and after a flight, which causes stress and wear on the metal parts, generating a solidifying force in its joining partners that is unknown.

Nowadays, objectives such as components reuse, remanufacture and recycling of components constitute some important reasons for the product disassembly. Nevertheless, industrial wastes such as in automotive industry are simply scrapped (dismantling, shredding and sorting) because it is currently too expensive to recover them [3]. However, there are few partially automated cases such as disassembly of electronics components [4], the disassembly process is feasible if the products contains valuable material such as gold or is large such as trains, aircrafts, and power lines because they have high value in the disassembly [5].

Disassembly is formally defined as the systematic separation of components and can be categorized into several types, such as destructive or non-destructive and partial (selective) or complete (full) disassembly [6]. The choice of separation procedures dependents mainly on the types of connections between the components, such as components joining (welding, screwing, solidifying) or component contact (filling, inserting) that require complex or simply separation operations, respectively. Generally, if the objective is to reuse the product, non-destructive disassembly technology is preferred because destructive disassembly is an irreversible operation. This paper focuses on the non-destructive disassembly of components with solidified connection as part of an environment friendly manufacturing.

Peer-review under responsibility of the scientific committee of the 11th CIRP Conference on Intelligent Computation in Manufacturing Engineering.

Despite that a high quality is required in the aviation industry, there are disassembly difficulties promotes that the process will be still largely manual in nature, the problem is attributed to several parameters such as the force and time to perform a task, the degree of precision, and accessibility to reach the product [7]. Furthermore, many disassembly control systems are not yet developed because they have limits due to their high uncertainty created by the nonuniformity of returned product models [4]. To overcome these limitations and develop an automation to the disassembly process, it is essential to reduce costs and improve working conditions within the industries. However, the main obstacle to disassembly of turbine blades is the uncertainty of the value of the disassembly force to provide the correct control action, therefore, we introduce a friction model to estimate this force.

The automated disassembling may not be as flexible as a manual disassembling. Nevertheless, if the product require high quality or has a high value as in turbine blades then the development of disassembly automation is necessary. In this work a piezo stack actuator is used to take advantage of the vibration force to reduce the amplitude of the force applied and the risk of damage in the actuator and final product, consequently, obtained more quality. Finally, disturbance is introduced to compensate the estimation error and test the robustness of the controller.

2. Related Work

Disturbance in control systems is created by different factors such as linearity and accuracy of the sensor or actuator, affecting controller performance. Despite the technological development in which controllers have been submerged, fields such as the robotics and teleoperation have relative disadvantages in their operation due to problems directly related to force control, many of these are due to aspects that have to do with the non-linear behaviour of the system, the force control of robots with the environment in which they operate have been one of the problems that are most investigating, some solutions are the implementation of new advanced control strategies that significantly improve robustness [8] and another is work with the model Therefore, a correct model is essential for the design of force controllers. In this topic the Lugre friction model is developed to reproduce the characteristics of the process.

PID controllers are widely used in many industrial processes and recently in other fields such as for the control and damp of the vibrations generated in smart structures in where e.g. one solution has been the implementation of an active vibration control based on PID algorithm and using the piezoelectric bounded [9]. However, finding the right control gains is important to satisfying and robust performance. For this topic a PID controller is implemented with its control gains defined for a quick process.

One of the purposes of the controller design is to extend actuator life, much of the damages are caused by rapid variations and by keeping them working at saturation points. The piezo stack actuator is designed to work with frequency, so it will not be damaged by abrupt variations, but if it is used at saturation points will suffer damage by mechanical wear. This can be avoided by reducing the amplitude of the force applied and compensating it with shock force, which will also cause the product to suffer less damages [10].

3. Friction model

3.1. Solidification

Although materials with high mechanical strength and corrosion resistance are placed in the aircraft engine due to the operational loads it has to withstand, there is an additional reaction force created for solidification between the turbine blades and the turbine disk. The assembly connections (connections which produces the desired microstructure in the bond region) [11] strongly define the disassembly characteristics of the turbine blades. Despite that assembly force is known, the disassembly force is unknown due to the working conditions to which they were subjected, such as high temperatures and pressures created by centrifugal forces acting on the blades during operation [11] generating solidification in the joining components.

Therefore, the reaction force denominated solidifying force $R_z(\mathrm{t},\mathrm{z})$ is completely unknown, however, it can be compared and modelled with another physical phenomenon such as the friction.

Figure 1 shows the development of this process. A piezo actuator applies the disassembly force $F(\mathrm{t},\mathrm{z})$ producing the displacement of the turbine blade position z(t) in the disc and the blade motion is defined for the distance Δ_z in the guide lf. If the distance Δ_z is smaller, then the turbine blade will have less risk of damage .which can be achieve by decreasing the force amplitude, consequently the duration of the impact will be reduced. A vibration controller is therefore necessary.

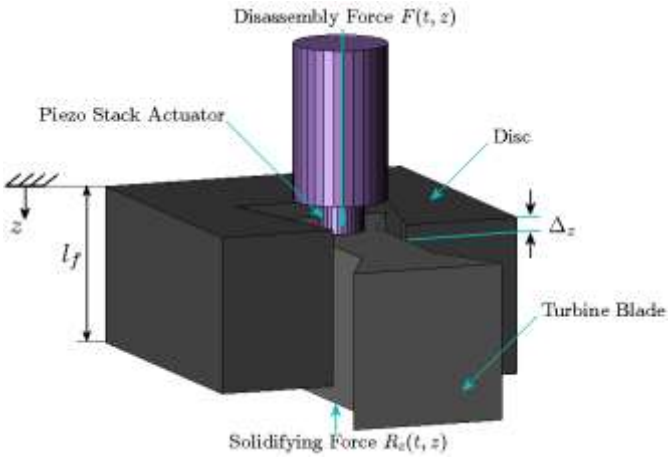

Fig. 1. Simplified model of disassembly task.

3.2. Lugre Friction Model

Despite solidifying force is still unknown, its behaviour is described by a friction model with unknown parameter. Friction opposes motion and is created by microscopic imperfections and irregularities of two surfaces in contact with each other. Further it is present in mechanical systems

that involve parts in contact. These characteristics are important for establishing the estimation of solidification behaviour. Many efforts have been made to develop an efficient friction model that contains all the features in regions I, II and III that correspond to static, transient and dynamic cases respectively. Fig 2b shows these regions, region II is the most complicated to model. However, Lugre model friction achieves this.

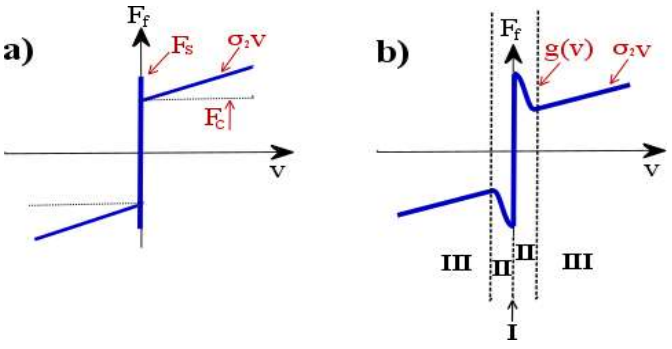

Fig. 2. Representation of friction behaviour with its regions (a) Coulomb Friction F_c , Stiction Friction F_s and viscous friction σ_2 ; (b) Lugre model with Stribeck curve in the sliding regime with function $g(v)$ y σ_2 .

When the contact of two surfaces at microscopic level is visualized, irregularities due to the presence of roughness are observed. The Lugre model proposes to describe it as when two rigid bodies come into contact through elastic bristles [12] (see figure 3); (for more information see [13]). The behaviour is described by

$$F_f = k_e \cdot z + c \cdot \frac{dz}{dt} \tag{1}$$

$$\frac{dz}{dt} = v - \frac{|v|}{g(v)} \cdot z \tag{2}$$

$$g(v) = F_C + (F_S - F_C)\, e^{-\left(\frac{v}{v_S}\right)^2} \tag{3}$$

Where F_f is the friction, is stiffness of the bristles, c is damping of the bristles, σ_2 represents the coefficient of viscous friction, v is the relative velocity between the two bodies, z is the average deflection of bristles, F_C is the coulomb force, F_S is the stiction force (break-away friction) and v_S is the velocity of Stribeck. For constant velocities, the steady-state friction is indicated by F_{SS} associated with velocity and is given by

$$F_{SS} = g(v) \cdot \mathrm{sgn}(v) + \sigma_2 \cdot v$$

$$= F_C \cdot \mathrm{sgn}(v) + (F_S - F_C) \cdot e^{\left(\frac{v}{v_S}\right)^2} \cdot \mathrm{sgn}(v) + \sigma_2 \cdot v \tag{4}$$

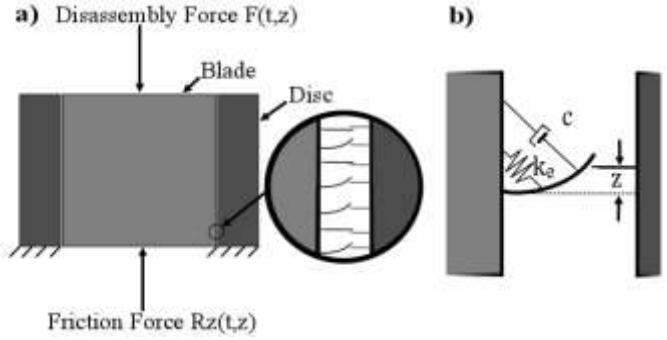

Fig. 3. Microscopic behaviour of the Lugre friction model (a) Bristles to describe the solidification; (b) Average deflection of the bristles.

Figure 3b shows the average deflection of the bristles for region I (compare Fig. 2b). If the force applied does not exceed the stiction force, the reaction force is defined by region I. The turbine blade will begin to slide, if the force applied exceeds the stiction force F_s , it will begin to enter region II and consequently region III. These regions show that the bristles become over-deflected generating disassembly motion, and the random behaviour of this phenomenon is captured by the behaviour of the bristles [12]. For our research, it is necessary to modify certain parameters of the Lugre friction model. The contact surface during disassembly of the turbine blade decreases from a maximum value until reaching the disassembling (Fig. 4), then the coulomb force F_C and the stiction force F_S will be smaller and will depend on the position of the blade z(t) , therefore the friction force $R_z(t,z)$ is proportional to the contact area [13], which is described by equations (5) and (6), and is shown in the figure 4.

$$F_S(z) = \left(\frac{m \cdot g - F_{SO}}{l_f}\right) \cdot z(t) + F_{SO} \tag{5}$$

$$F_C(z) = \left(\frac{m \cdot g - F_{CO}}{l_f}\right) \cdot z(t) + F_{CO} \tag{6}$$

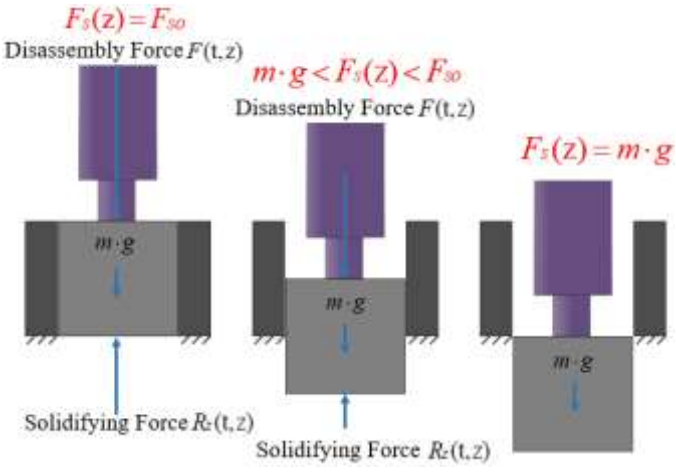

Fig. 4. Reduction of the Stiction Force $F_s(z)$ due to increased displacement.

where F_{so} and F_{co} represent the initial values of the stiction and coulomb forces respectively and m is the mass of the turbine blade. Therefore, equations (1) and (4) are modified for the estimation of the solidification by equations (7) and (8), due to the speed of the system, the viscous friction not is considered σ_2 .

$$R_z(\mathrm{t},\mathrm{z}) = k_e \cdot z(\mathrm{t}) + c \cdot \frac{dz(\mathrm{t})}{dt} \tag{7}$$

$$R_{zz}(\mathrm{t},\mathrm{z}) = F_c(\mathrm{z}) \cdot \mathrm{sgn}(v) + \left(F_s(\mathrm{z}) - F_c(\mathrm{z})\right) \cdot e^{-\left(\frac{v}{v_s}\right)^2} \cdot \mathrm{sgn}(v) \tag{8}$$

The parameters chosen for the simulation have been multiplied and modified slightly with a high gain compared to those proposed by [12]. These are defined by table I.

Table 1. Parameters for Simulation of the Lugre Friction Model.

Name	Symbol	Value	Unit
Initial stiction friction	F_{so}	450	$[N]$
Initial coulomb friction	F_{co}	360	$[N]$
Stiffness coefficient	k_e	30000000	$[N/m]$
Damping coefficient	c	$1,6 \cdot k_e$	$[N \cdot s/m]$
Stribeck velocity	v_s	0.09	$[m/s^2]$
Total disassembly distance	l_f	0.1	$[m]$
Mass	m	1	$[kg]$

The friction force of the Lugre model does not represent the real value of the solidifying force because the estimation is analytical for trying to know the reality. Therefore, for describing this inaccuracy, the friction force is multiplied by a random number $(1 \pm \mathrm{var})$ creating a disturbance defined for the variable var (compare Fig. 5). The friction force can take any value from $\left(1 - \mathrm{var}\right) \cdot R_z(\mathrm{t},\mathrm{z})$ to $\left(1 + \mathrm{var}\right) \cdot R_z(\mathrm{t},\mathrm{z})$.

Figure 5 shows the system block diagram. To obtain the position of the displacement z(t) , the second Newtonian law applies to the relative force $F_t(\mathrm{t},\mathrm{z})$.

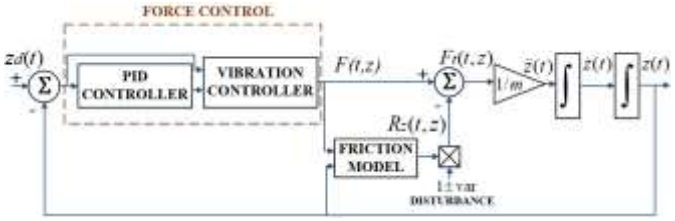

Fig. 5. Block Diagram of Control System.

4. Force Controller Design

The design of the controller is based on pole analysis of the closed loop system transfer function. Therefore, it is necessary to reduce the blocks diagram, however, there is a high degree of difficulty when working with the Stribeck effect (compare with the region II in Fig. 2b) in the Laplace domain. Although the Stribeck curve gives a perspective of the transition between static friction and dynamic friction rather than a discontinuous fall, to facilitate the work of the control design, it is necessary to eliminate this effect and use the equation (9). Figure 2a shows the friction behaviour for the controller design.

$$R_Z(\mathrm{t},\mathrm{z}) = \begin{cases} k_e \cdot z(\mathrm{t}) + \mathrm{c} \cdot \dfrac{dz}{dt} & if \quad F(\mathrm{t},\mathrm{z}) \le F_S \\ F_C(\mathrm{z}) & if \quad F(\mathrm{t},\mathrm{z}) > F_S(\mathrm{z}) \end{cases} \tag{9}$$

4.1. PID Controller Design

For the calculation of the PID controller gains, only are taken into account the regions I and III defined for equation (9) corresponding to static and dynamic cases respectively. The transfer function $T_S(s)$ for the static case is given by the following equation:

$$T_S(s) = \frac{\dfrac{kd_s}{m} \cdot s^2 + \dfrac{kp_s}{m} \cdot s + \dfrac{ki_s}{m}}{s^3 + \left(\dfrac{c + kd_s}{m}\right) \cdot s^2 + \left(\dfrac{k_e + kp_s}{m}\right) \cdot s + \dfrac{ki_s}{m}} \tag{10}$$

where kp_s , kd_s and ki_s are the proportional, derivative and integral gains respectively for the static case.

To reduce the level of complexity of third order system analysis, it is compared with a stable second order system multiplied by a pole located in a stable zone given by equation (11).

$$P(s) = \left(s + a\right) \cdot \left(s^2 + 2 \cdot \varepsilon \cdot \omega + \omega^2\right) \tag{11}$$

where a is the pole in stable zone, ω is the natural frequency of the system and ε is the damping coefficient of the system. Equalizing the equations (10) with (11), the tuning constants are obtained:

$$kp_s = \left(\omega^2 + 2 \cdot a \cdot \varepsilon \cdot \omega + \omega^2\right) - k_e,$$
$$kd_s = \left(2 \cdot \varepsilon \cdot \omega + a\right) \cdot m - \varepsilon, \quad ki_s = a \cdot \omega^2 \cdot m$$

For the analysis in the dynamic case, an initial condition exists and is as follows: The disassembly force $F(\mathrm{t},\mathrm{z})$ and the friction force $R_z(\mathrm{t},\mathrm{z})$ have already reached the stiction force and instantaneously the last mentioned will be equal to the coulomb force $F_c(\mathrm{z})$. This is increasingly smaller depending on the position and is described as a force gain in the blocks diagram which is inversely proportional to the coulomb force $F_c(\mathrm{z})$ given by the equation (12).

$$m_2 = \frac{F_{CO} - m \cdot g}{l_f} \tag{12}$$

Its transfer function $T_d(s)$ is given by:

$$T_d(s)=\frac{\frac{kd_d\cdot m_2}{m}\cdot s^2+\frac{kp_d\cdot m_2}{m}\cdot s+\frac{ki_d\cdot m_2}{m}}{s^3+\left(\frac{kd_d\cdot m_2}{m}\right)\cdot s^2+\left(\frac{1+kp_d}{m}\right)\cdot m_2\cdot s+\frac{ki_d\cdot m_2}{m}} \quad (13)$$

where kp_d, kd_d and ki_d are the proportional, derivative and integral gains respectively for the dynamic case. In a situation similar to that of the static case when equations (11) and (12) are equalised, the tuning constants are given by:

$$kp_d=\frac{\left(\omega^2+2\cdot a\cdot\varepsilon\cdot\omega\right)\cdot m}{m_2}-1,$$

$$kd_d=\frac{\left(2\cdot\varepsilon\cdot\omega+a\right)\cdot m}{m_2},\quad ki_d=\frac{a\cdot\omega^2\cdot m}{m_2}$$

The control parameter ε and ω for static and dynamic cases are defined for a quick process, the location of the introduced pole is in $a=200$, and to obtain ω is necessary to consider the settling time at 2% given by $t_s=4/\varepsilon\cdot\omega$, where $t_s=0,0005$ [s] and $\varepsilon=1$. The response velocity causes the control actions (disassembly force) remain close to the coulomb force, for which it is necessary to pay attention to dynamic gains, then the final tuning gains are given by:

$$kp_d=0,1\cdot kp_s+0,9kp_d,$$

$$kd_d=0,1\cdot kd_s+0,9kd_d,\quad ki_d=0,1\cdot ki_s+0,9ki_d$$

4.2. Vibration Controller Design

To work with vibration it is necessary to modify the control parameters $\varepsilon=1,2$ and $t_s=0,00052$ [s] for obtaining a gentler response. Moreover, vibration control uses the FM modulation principle, where the input amplitude is that of the PID controller output and the modulation parameter is the error (compare figure 6).

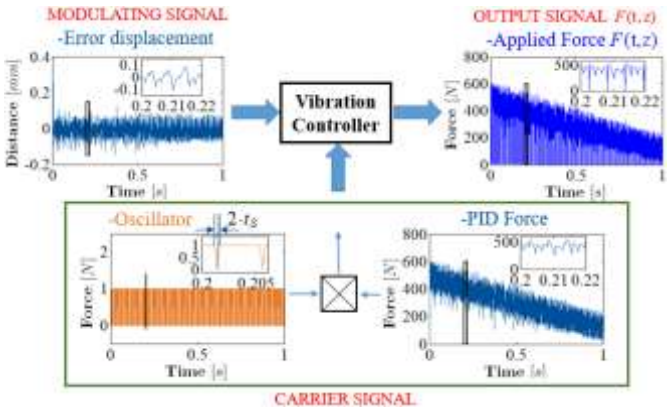

Fig. 6. Vibration controller based in FM modulation.

The output frequency will be proportional to the amount of error, furthermore to reduce even more amplitude the pulse-width below is the least possible. In addition, in simulation it is essential to be careful with aliasing phenomena and apply the Nyquist criterion to establish model frequency, sampling frequency, vibration frequency range, etc. This is why the control frequency ranges from 80[Hz] to 160[Hz].

5. Results

The table II shows the PID controller gains (x1000) for the implementation of the force controller with and without vibration, where in both cases the dynamic ratio prevails, and the integral gains are too high to achieve a quick response.

Table 1. Parameters for Simulation of the Lugre Friction Model.

Description	Control without Vibration			Control with Vibration		
	Static	Dynamic	Total	Static	Dynamic	Total
Proportional Gain	31200	19,2	3137,3	8168,3	12,6	828,2
Derivative Gain	7,2000	0,0046	0,7242	6,5846	0,0044	0,6625
Integral Gain	12800000	3655	1283289	8218277	2347	823940

5.1. Force Control

Figure 7 shows the solidifying force $R_z(t,z)$ with a disturbance range of ±5% when applying a force control $F(t,z)$.

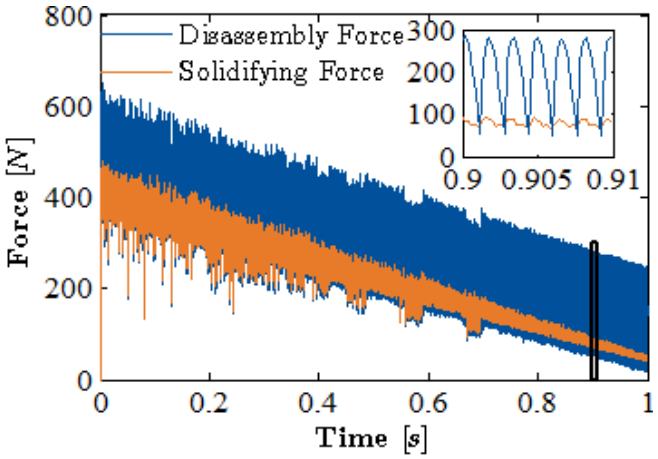

Fig. 7 Control and Solidifying Forces with disturbance range of±5%.

5.2. Force Control with Vibration

Figure 8 shows the solidifying force $R_z(t,z)$ with a disturbance range of ±5% when applying a force control with vibration $F(t,z)$. Figure 9 shows the final results of the two controllers. The force applied with vibration is smoother than the force applied without vibration However, this difference is imperceptible and despicable.

Figure 10 shows the errors defined by the absolute error integral (IAE) that is used for performance comparison to present results in each interaction with different variation ranges until before the controller allows an unstable response. For the control without vibration its maximum disturbance

range is ±12.5% while for the vibration control its range is ±8.5%.

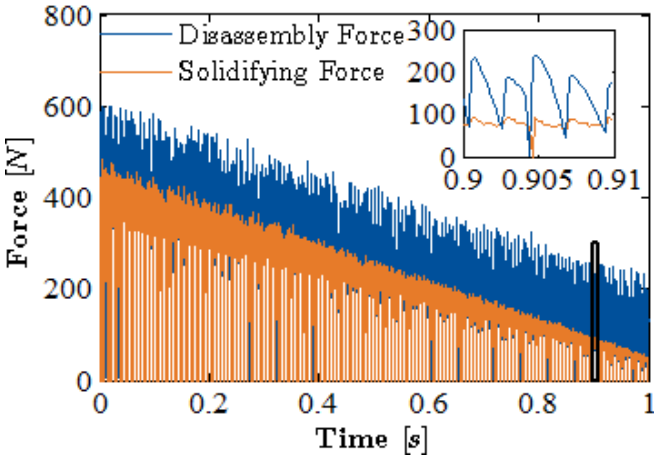

Fig. 8 Vibration Control and Solidifying Force with disturbance range of±5%.

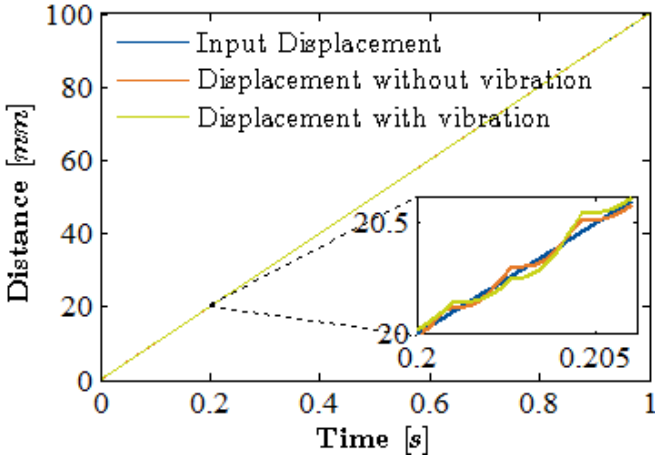

Fig. 9 Desired and Measured Displacements with and without Vibration Control.

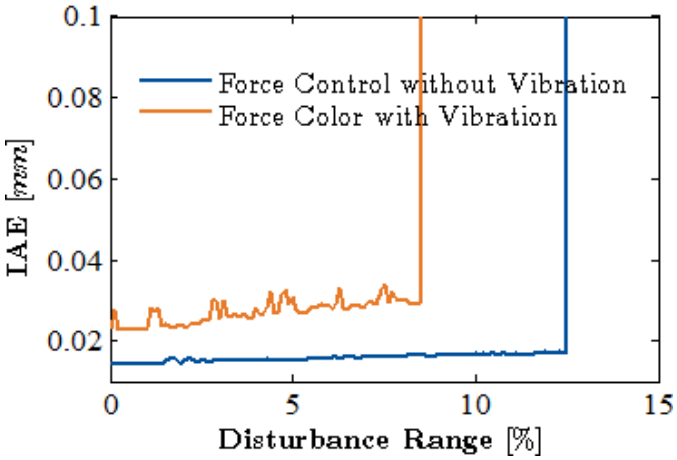

Fig. 10. Error results of the force controller with and without vibration and disturbance ranges

6. Conclusions

Solidification is an undesired phenomenon in disassembly that is present in component joining due to the operation factors, causing difficulty in knowing the reaction force and therefore for the development of a disassembly automation system for turbine blades. This force was calculated with the Lugre friction model and was used for the development a force controller formed for a PID controller and a vibration controller. The first was implemented to apply a correct disassembly force with the calculation of its gains tuning based on the poles analysis of static and dynamic cases, further the control parameters were designed to obtain a quick response and the desired displacement, creating a high quality disassembly process. Furthermore, wear on the piezo actuator was reduced by decreasing the applied force amplitude with the implementation of vibrations control based on FM modulation.

Disturbance is an unwanted signal that affects the process operation. In this topic, disturbance in solidifying force was introduced to compensate the estimation error, so several tests have been introduced with different disturbance values that have been progressively increased and analyzed with the Integral Absolut Error (IAE). Finally, the simulation is implemented with Simulink/MATLAB using the Simmechanics toolbox, obtaining excellent results up to a maximum acceptable disturbance range.

References

[1] J.R. Duflou, G. Seliger, S. Kara, Y. Umeda, A. Ometto, B. Willems, Efficiency and feasibility of product disassembly: A case-based study, In CIRP Annals, Volume 57, Issue 2, 2008, Pages 583-600.
[2] Eylem Asmatulu, Michael Overcash, and Janet Twomey, “Recycling of Aircraft: State of the Art in 2011,” Journal of Industrial Engineering, vol. 2013, Article ID 960581, 8 pages, 2013.
[3] Katja Tasala Gradin, Conrad Luttropp, Anna Björklund, Investigating improved vehicle dismantling and fragmentation technology, In Journal of Cleaner Production, Volume 54, 2013, Pages 23-29.
[4] M. Merdan, W. Lepuschitz, T. Meurer and M. Vincze, "Towards ontology-based automated disassembly systems," IECON 2010 - 36th Annual Conference on IEEE Industrial Electronics Society, Glendale, AZ, 2010, pp. 1392-1397.
[5] Åkermark AM. (1997) Design for Disassembly and Recycling. In: Krause FL., Seliger G. (eds) Life Cycle Networks. Springer, Boston, MA.
[6] M.M.L. Chang, S.K. Ong, A.Y.C. Nee, Approaches and Challenges in Product Disassembly Planning for Sustainability, In Procedia CIRP, Volume 60, 2017, Pages 506-511.
[7] Anoop Desai, Anil Mital, Evaluation of disassemblability to enable design for disassembly in mass production, In International Journal of Industrial Ergonomics, Volume 32, Issue 4, 2003.
[8] E. Sariyildiz and K. Ohnishi, "A comparison study for force sensor and reaction force observer based robust force control systems," 2014 IEEE 23rd International Symposium on Industrial Electronics (ISIE), Istanbul, 2014, pp. 1156-1161.
[9] Shunqi Zhang, Rüdiger Schmidt, Xiansheng Qin, Active vibration control of piezoelectric bonded smart structures using PID algorithm, In Chinese Journal of Aeronautics, Volume 28, Issue 1, 2015, Pages 305-313.
[10] Julius Wolff, Miping Yan, Melf Schultz, Annika Raatz, Reduction of Disassembly Forces for Detaching Components with Solidified Assembly Connections, In Procedia CIRP, Volume 44, 2016, Pages 328-333.
[11] Lane C. (2014) Introduction. In: The Development of a 2D Ultrasonic Array Inspection for Single Crystal Turbine Blades. Springer Theses (Recognizing Outstanding Ph.D. Research). Springer, Cham.
[12] C. Canudas de Wit, H. Olsson, K. J. Astrom and P. Lischinsky, "A new model for control of systems with friction," in IEEE Transactions on Automatic Control, vol. 40, no. 3, pp. 419-425, Mar 1995.
[13] K. Johanastrom and C. Canudas-de-Wit, "Revisiting the LuGre friction model," in IEEE Control Systems, vol. 28, no. 6, pp. 101-114, Dec. 2008.